Electronic Supplementary Material (ESI) for RSC Advances.
This journal is © The Royal Society of Chemistry 2019

Electronic Supplementary Information

Planar Graphitic ZnS, Buckling ZnS Monolayers and Rolled-up Nanotubes as Nonlinear Optical Materials: First-Principles Simulation

Lei Hu[1*], Wencai Yi[2], Jianting Tang[1], Tongde Rao[1], Zuju Ma[3], Chuanbo Hu[1], Lei Zhang Tingzhen Li[1 *]

[1]School of Environmental and Chemical Engineering, Chongqing Three Gorges University, Chongqing, 404100, China

[2]Laboratory of High Pressure Physics and Material Science, School of Physics and Physical Engineering, Qufu Normal University, Qufu, 273165, China

[3]School of Materials Science and Engineering, Anhui University of Technology, Maanshan, 243 002, China

Email: huleisanxu@163.com, leihu@sanxiau.edu.cn, litingzhen@163.com

Keywords: planar ZnS monolayer; buckling ZnS monolayer; ZnS single-walled nanotube; second harmonic generation; nonlinear optical property; first-principles; mid-infrared

1. Band structure and interlayer distance of wurtzite ZnS

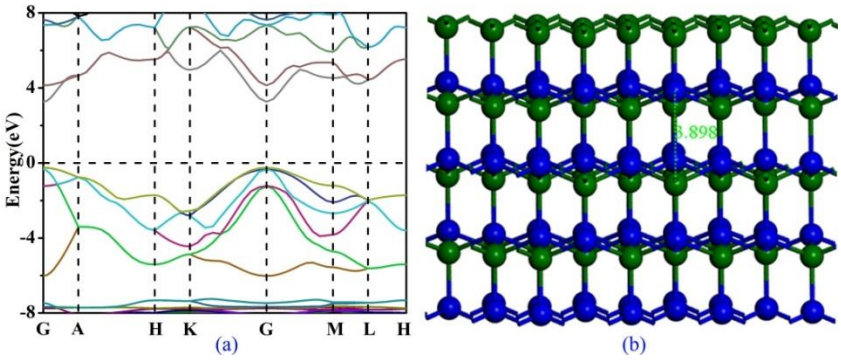

Figure S1 (a) band structure calculated with HSE06 functional and (b) interlayer distance of wurtzite ZnS

As can be seen, wurtzite ZnS crystal exhibits a direct bandgap, with the VBM and CBM both

located at the Γ (0.0, 0.0, 0.0) point. The band gap of wurtzite ZnS crystal is 3.51 eV, which is close to the experimental value 3.77 eV [1]. As shown in Figure 1S(b), similar to planar g-SiC [2], the effective thickness of planar g-ZnS is set as the interlayer distance 3.898 Å of wurtzite ZnS crystal.

2. Band structure of planar g-ZnS

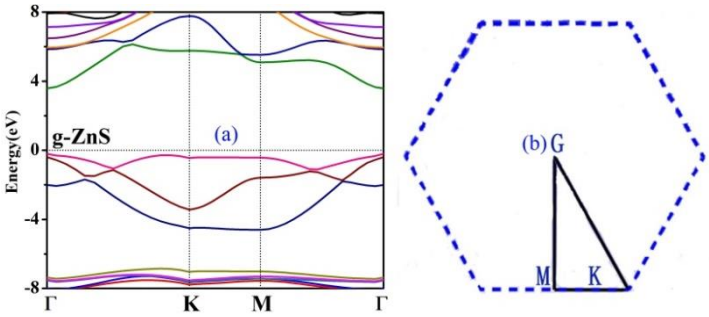

Figure S2 (a) Band structure of planar g-ZnS monolayer calculated using HSE06 functional, and (b) high symmetry k-point path in the Brillouin zone path Γ (0, 0, 0) → K (-1/3, 2/3, 0) → M (0, 1/2, 0) → Γ (0, 0, 0).

As suggested by Figure S2, planar g-ZnS monolayer has a direct band gap of 3.80 eV at the Γ point.

3. Band structure of buckling R-ZnS monolayer

Figure S3 suggests buckling R-ZnS monolayers have direct bandgaps with the VBM and CMB located at the Γ point. The bandgaps of buckling R-ZnS are steady around 3.90 eV with a small variance of ~ 0.10 eV.

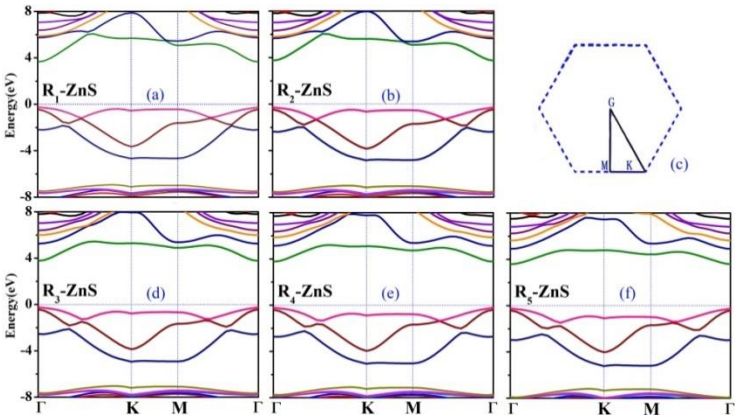

Figure S3 Band structure of buckling R_1-ZnS, R_2-ZnS, R_3-ZnS, R_4-ZnS and R_5-ZnS calculated using HSE06 functional. The high symmetry k-point path in the Brillouin Zone, as shown in (c), is chosen as Γ (0, 0, 0) → K (-1/3, 2/3, 0) → M (0, 1/2, 0) → Γ (0, 0, 0).

4. Band structure and total density of electronic states of a representative (12, 0) ZnS SWNT

Zigzag and chiral ZnS SWNTs show similar electronic structures. As a representative, the band structure and total density of electronic states are given in Figure S4. As can be seen, ZnS (12, 0) SWNT exhibits a direct band gap at the Γ (0.0, 0.0, 0.0) point, and a sharp peak in the top of valence bands.

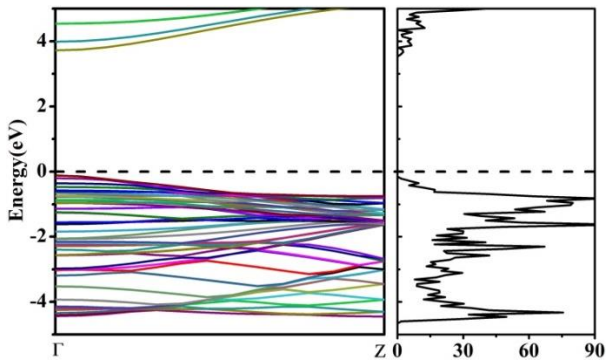

Figure S4 Band structure and total density of electronic states of a (12, 0) ZnS SWNT

5. SHG intensity estimation of planar g-ZnS, buckling R-ZnS and ZnS SWNTs

According to the electric dipole theory, the SHG intensity $I_{2\omega}$ is proportional to $\frac{[\chi^{(2)}]^2 d^2 \omega^2}{n_\omega n_{2\omega}^2}$, where d is the effective thickness of monolayers, n_ω and $n_{2\omega}$ are respectively the refractive index at frequency ω of excitation laser and at frequency 2ω of SHG field [3]. Previous experiments demonstrate the nonresonant SHG intensity of monolayer GaSe is stronger than that of monolayer MoS_2, WS_2, WSe_2 and BN [3]. Here, we make a comparison of SHG intensities of monolayer g-ZnS, GaSe and MoS_2. The theoretical n_ω, $n_{2\omega}$ at 1600 nm and effective thickness of planar g-ZnS in Table S1, and that of monolayer GaSe [4] and MoS_2 [3] is also shown for comparison. The theoretical SHG coefficients $\chi_{xxy}^{(2)}$ at an excitation wavelength of 1600 nm for monolayer GaSe and planar g-ZnS are 75 pm/V [4] and 42 pm/V, respectively. The estimated ration of SHG intensities at 1600 nm between monolayer g-ZnS and GaSe is ~0.2. Experiments show the SHG intensity of single-layer MoS_2 at 1600 nm is less than 1/10 that of single-layer GaSe [3]. Therefore, the nonresonant SHG

intensity of planar g-ZnS at 1600 nm is stronger than that of single-layer MoS_2, which mainly originates from smaller optical refractive indices of planar g-ZnS.

Table S1. n_ω, $n_{2\omega}$ at 1600 nm and effective thickness d (Å) of monolayer GaSe, planar g-ZnS, MoS_2 and buckling R-ZnS

Materials	GaSe	g-ZnS	MoS_2	R_1-ZnS	R_2-ZnS	R_3-ZnS	R_4-ZnS	R_5-ZnS
d	7.99	3.90	6.0	3.92	3.93	4.18	4.25	4.35
n_ω	2.70	2.15	4.0	2.16	2.16	2.15	2.16	2.17
$n_{2\omega}$	2.77	2.18	4.5	2.19	2.19	2.17	2.18	2.20

As shown in Figure 2 of the main manuscript, the SHG coefficient of planar g-ZnS nearly keeps constant from zero to 1.0 eV, e.g. 42 pm/V at 1600 nm versus 37.4 pm/V at the static limit, which indicating their nonresonant SHG intensities nearly keep constant. Moreover, the nonresonant SHG regime of planar g-ZnS covers the whole mid-infrared regime (2-8 μm), so planar g-ZnS has a potential application in the mid-infrared regime.

Table S2. n_ω and $n_{2\omega}$ at 1600 nm of ZnS SWNTs

Materials	(6, 0)	(8,0)	(9,0)	(12,0)	(16,0)	(18,0)	(20,0)	(4,2)	(6,3)
n_ω	2.15	2.16	2.15	2.15	2.16	2.14	2.13	2.16	2.17
$n_{2\omega}$	2.19	2.20	2.18	2.19	2.20	2.17	2.16	2.19	2.21

Furthermore, the optical refractive indices n_ω and $n_{2\omega}$ of buckling R-ZnS [cf. Table S1] and ZnS SWNTs [cf. Table S2] are nearly not modified in comparison with that of planar g-ZnS. Resultantly, small refractive indices will also enhance SHG signals of buckling R-ZnS and ZnS SWNTs.

References

1. J. X. Ding, J. A. Zapien, W. W. Chen, Y. Lifshitz, S. T. Lee and X. M. Meng, *Lasing in ZnS nanowires grown on anodic aluminum oxide templates*, *Appl. Phys. Lett.*, 2004, **85**, 2361.
2. I. J. Wu and G. Y. Guo, *Second-harmonic generation and linear electro-optical coefficients of SiC polytypes and nanotubes*, *Phys. Rev. B*, 2008, **78**, 035447.
3. X. Zhou, J. Cheng, Y. Zhou, T. Cao, H. Hong, Z. Liao, S. Wu, H. Peng, K. Liu and D. Yu, *Strong Second-Harmonic Generation in Atomic Layered GaSe*, *J. Am. Chem. Soc.*, 2015, **137**, 7994.

4. L. Hu, X. Huang and D. Wei, *Layer-independent and layer-dependent nonlinear optical properties of two-dimensional GaX (X = S, Se, Te) nanosheets*, *Phys. Chem. Chem. Phys.*, 2017, **19**, 11131.